Table 1. Detection of hGH in grafted epidermis generated from transduced keratinocytes. Epidermis generated by transduced keratinocytes was harvested 7 to 8 days after grafting, snap-frozen in liquid nitrogen, and powdered. The powder was suspended in 300 μl of 25 m*M* tris buffer (*p*H 7.5), containing 1 m*M* EDTA, and sonically disrupted for 10 seconds at 50 W. The suspension was centrifuged for 5 minutes at 15,000*g*, and the supernatant was assayed for hGH by RIA. YF17 no. 1 and no 2 are control samples of human epidermis generated by uninfected keratinocytes.

Strains	Amount of hGH per graft (ng)	Area of graft (mm^2)
Control		
YF17 no. 1	0	240
YF17 no. 2	0	140
Experimental		
YF19 DOL-hGH	5.6	160
YF17 DOL-hGH	4.0	200

The feasibility of delivering a secreted protein by skin grafting will depend not only on the rate of its synthesis in the graft, but also on the efficiency of its transfer to the circulation. Although, it is known that even quite large proteins can pass in the reverse direction from the dermis into the epidermis (*13*), there is no information on the efficiency of transfer. Further research is being devoted to improved expression of hGH by the use of other retroviral constructs, and to the study of other secreted proteins assayable at lower concentration. In this way we should be able to definitively assess the feasibility of hormone delivery by skin grafting.

REFERENCES AND NOTES

1. J. G. Rheinwald and H. Green, *Cell* **6**, 331 (1975).
2. G. G. Gallico III, N. E. O'Connor, C. C. Compton, O. Kehinde, H. Green, *N. Engl. J. Med.* **311**, 448 (1984).
3. R. D. Cone and R. C. Mulligan, *Proc. Natl. Acad. Sci. U.S.A.* **81**, 6349 (1984).
4. C. L. Cepko, B. E. Roberts, R. C. Mulligan, *Cell* **37**, 1053 (1984); A. J. Korman, J. D. Frantz, J. L. Strominger, R. C. Mulligan, *Proc. Natl. Acad. Sci. U.S.A.* **84**, 2150 (1987).
5. D. A. Williams, I. R. Lemischka, D. G. Nathan, R. C. Mulligan, *Nature (London)* **310**, 476 (1984).
6. R. Mann, R. C. Mulligan, D. Baltimore, *Cell* **33**, 153 (1983).
7. S. W. Kessler, *Methods Enzymol.* **73B**, 442 (1981).
8. U. J. Lewis *et al.*, *Human Growth Hormone*, S. Raiti and R. A. Tolman, Eds. (Plenum, New York, 1986), pp. 439–447; J. B. Martin, *ibid.*, p. 303.
9. M. Morikawa, T. Nixon, H. Green, *Cell* **29**, 783 (1982).
10. H. Green, O. Kehinde, J. Thomas, *Proc. Natl. Acad. Sci. U.S.A.* **76**, 5665 (1979).
11. Y. Barrandon, V. Li, H. Green, in preparation.
12. D. Jähner *et al.*, *Nature (London)* **298**, 623 (1982).
13. R. E. Nordquist, R. L. Olson, M. A. Everett, *Arch. Dermatol.* **94**, 482 (1966); E. Schreiner and K. Wolff, *Arch. Klin. Exp. Dermatol.* **235**, 78 (1969).
14. A. P. Feinberg and B. Vogelstein, *Anal. Biochem.* **132**, 6 (1983).
15. The antiserum to hGH NIAMDD [anti-hGH-1 (AFP-4793B)] was obtained from the National Institute of Diabetes and Digestive and Kidney Diseases.
16. We thank H. Goodman for the complementary DNA encoding hGH, and C. Compton for providing histological sections and advice. We thank Genentech, Inc., for the cloned hGH used for controls, and Chiron, Inc., for the cloned human EGF used for cultivation of keratinocytes and 3T3-F442A cells. Supported by NIH grants CA38497 (R.C.M.), CA26712 (R.C.M.), CA40029 (H.G.), and GM33158 (H.G.) and a postdoctoral fellowship from the Cancer Research Institute (J.R.M.)

30 March 1987; accepted 22 June 1987

Uromodulin (Tamm-Horsfall Glycoprotein): A Renal Ligand for Lymphokines

CATHERINE HESSION, JEAN M. DECKER, ANNE P. SHERBLOM, SATISH KUMAR, CHO C. YUE, ROBERT J. MATTALIANO, RICHARD TIZARD, ERIC KAWASHIMA, URSULA SCHMEISSNER, SHERYL HELETKY, E. PINGCHANG CHOW, CYNTHIA A. BURNE, ALAN SHAW, ANDREW V. MUCHMORE*

The protein portion of the immunosuppressive glycoprotein uromodulin is identical to the Tamm-Horsfall urinary glycoprotein and is synthesized in the kidney. Evidence that the glycoproteins are the same is based on amino acid sequence identity, immunologic cross-reactivity, and tissue localization to the thick ascending limb of Henle's loop. Nucleic acid sequencing of clones for uromodulin isolated from a complementary DNA bank from human kidney predicts a protein 639 amino acids in length, including a 24–amino acid leader sequence and a cysteine-rich mature protein with eight potential glycosylation sites. Uromodulin and preparations of Tamm-Horsfall glycoprotein bind to recombinant murine interleukin-1 (rIL-1) and human rIL-1α, rIL-1β, and recombinant tumor necrosis factor (rTNF). Uromodulin isolated from urine of pregnant women by lectin adherence is more immunosuppressive than material isolated by the original salt-precipitation protocol of Tamm and Horsfall. Immunohistologic studies demonstrate that rIL-1 and rTNF bind to the same area of the human kidney that binds to antiserum specific for uromodulin. Thus, uromodulin (Tamm-Horsfall glycoprotein) may function as a unique renal regulatory glycoprotein that specifically binds to and regulates the circulating activity of a number of potent cytokines, including IL-1 and TNF.

UROMODULIN IS AN 85-KD IMMUNOsuppressive glycoprotein that was originally purified to homogeneity from urine of pregnant women on the basis of its inhibitory activity in vitro in an antigen-specific human T-cell proliferative assay (*1*). Subsequent studies demonstrated that uromodulin also inhibits the comitogenic effect of interleukin-1 (IL-1) on both C3H-HEJ thymocytes and the IL-1–responsive D10-G.4 cell line (*2*). By means of a solid-phase binding assay, it was shown that murine IL-1α is a high-affinity ligand for uromodulin with an estimated dissociation constant of $3 \times 10^{-10} M$ (*3*). Although uromodulin is enriched in urine from pregnant women, it has also been isolated from urine of normal male donors; however, uromodulin from the latter source exhibits lower levels of immunosuppressive activity in vitro (*4*). Since the immunosuppressive activity of uromodulin (i) is resistant to pronase digestion, (ii) is destroyed by periodate treatment, (iii) is resistant to a number of protein denaturation procedures, and (iv) can be recovered in the carbohydrate fractions released after digestion of uromodulin with *N*-glycanase, we have suggested that the carbohydrate portion of uromodulin plays a fundamental role in its biologic activity (*5*). Other work showing that oligosaccharides derived from uromodulin or even defined monosaccharides can compete with uromodulin for binding to IL-1 suggests that IL-1 is a "mammalian lectin" with specificity toward carbohydrate moieties on uromodulin (*6*). We now report further characterization of uromodulin, including its amino acid sequence and binding specificity.

Amino acid sequence analysis was performed with homogeneous uromodulin (*1*). In addition to the intact uromodulin polypeptide, tryptic fragments of both *S*-β-(4-pyridylethyl)-uromodulin (*S*-PE-uromodulin) and *N*-succinyl, *S*-PE-uromodulin were

C. Hession, R. J. Mattaliano, R. Tizard, E. Kawashima, U. Schmeissner, S. Heletky, E. P. Chow, C. A. Burne, A. Shaw, Biogen Research Corporation, Cambridge, MA 02142.
J. M. Decker, A. P. Sherblom, A. V. Muchmore, Metabolism Branch, National Cancer Institute, National Institutes of Health, Bethesda, MD 20892.
S. Kumar, University of Chicago, Pritzker School of Medicine, Chicago, IL 60637.
C. C. Yue, Case Western Reserve University, Cleveland, OH 44106.

*To whom reprint requests should be addressed.

prepared and subjected to automated Edman degradation (*7*). Individual samples (~700 pmol each) of either uromodulin or Tamm-Horsfall protein were reduced and alkylated (*7*). Succinylation, tryptic digestion, and peptide separations were performed as described (*8*), except that reversed-phase high-performance liquid chromatography was performed at a flow rate of 300 μl/min with a RP-300 column (2.1 by 220 mm, Brownlee) for tryptic peptides of *S*-PE-uromodulin and *S*-PE–Tamm-Horsfall protein. A BU-300 column (2.1 by 30 mm, Brownlee) was used for tryptic peptides of *N*-succinyl, *S*-PE-uromodulin. The sequences obtained by these analyses are shown in Fig. 1, where the corresponding regions for both uromodulin and Tamm-Horsfall are noted.

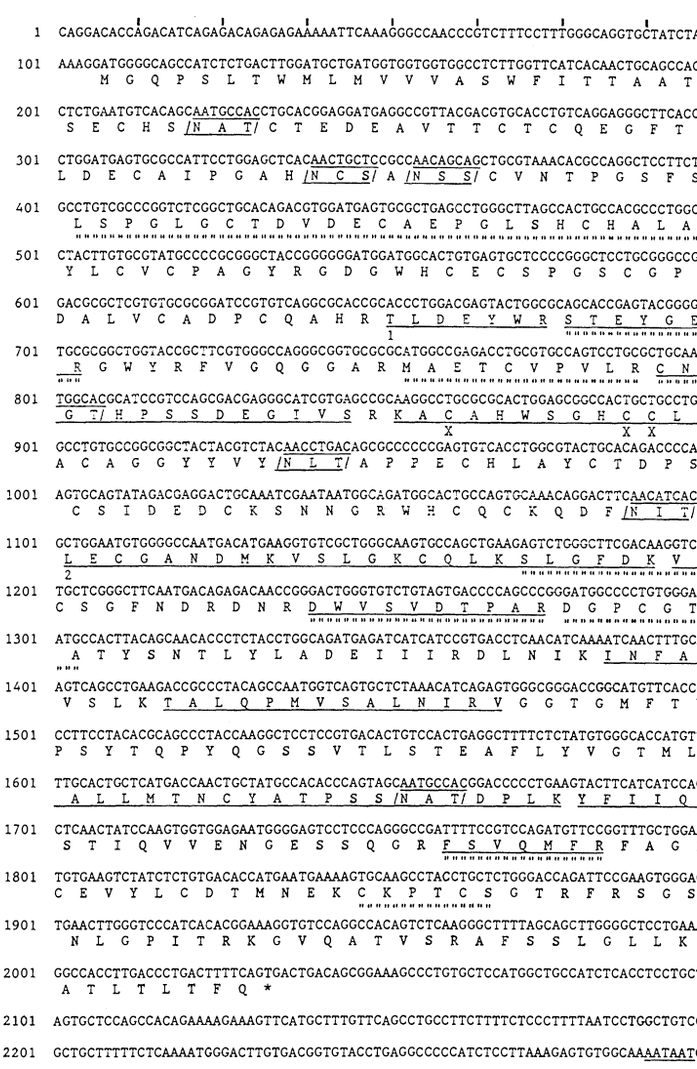

Fig. 1. Nucleotide and amino acid sequence of human uromodulin (Tamm-Horsfall glycoprotein). The coding strand of the composite cDNA sequence is displayed 5′ to 3′, with nucleotide +1 being the 5′ end of clone 6.7. Nucleic acid sequencing of a uromodulin genomic clone encompassing the 5′ region of the cDNA revealed no additional in-frame upstream methionine. The genomic sequence and the primer extension of the mRNA predict that the message initiates approximately 25 bases upstream from the first nucleotide of the cloned cDNA sequence. A modified polyadenylation signal, underlined, is located 20 bases upstream from the polyadenylation site (●) at nucleotide 2290. The nucleic acid sequence was obtained by the method of Maxam and Gilbert (*30*) and by modifications of the procedure of Church and Gilbert by Tizard and Nick (*31*). The predicted amino acid sequence is shown beneath the nucleic acid sequence. Peptides for which the amino acid sequence was obtained directly are denoted by either a solid line (——) (derived from uromodulin) or a hatched line (" " " ") (derived from Tamm-Horsfall glycoprotein). In several cases, identical peptides were sequenced for both protein preparations. X denotes those portions at which the identity of the amino acid could not be unambiguously determined by microsequence analysis. In two cases, these ambiguities were found within glycosylation consensus sites and are consistent with the occurrence of this posttranslational modification at these residues. The termination codon is indicated by an asterisk. The arrow indicates the apparent mature amino terminus of the polypeptide, preceded by a leader sequence. Amino terminal microheterogeneity observed during the Edman degradation precluded the exact determination of the mature amino-terminal amino acid. The boxed areas of the amino acid sequence indicate potential *N*-linked glycosylation sites. The amino acid sequence contains 48 cysteine residues. Abbreviations for the amino acid residues are: A, Ala; C, Cys; D, Asp; E, Glu; F, Phe; G, Gly; H, His; I, Ile; K, Lys; L, Leu; M, Met; N, Asn; P, Pro; Q, Gln; R, Arg; S, Ser; T, Thr; V, Val; W, Trp; and Y, Tyr.

When these studies began, it was not known that uromodulin is identical to Tamm-Horsfall protein. Because uromodulin was isolated and purified from urine of pregnant women, a tissue source of messenger RNA (mRNA) for complementary DNA (cDNA) cloning had to be identified. Utilizing the selective sequence data derived from tryptic peptides, we hybridized the antisense degenerate oligonucleotide probes UM1 and UM2 (Table 1) to a single 2400-nucleotide transcript on Northern blot analysis of human polyadenylated [poly(A)$^+$] RNA (*9*).

On the basis of this observation, a human kidney cDNA library was constructed in the Eco R5 site of pBR322 according to the method of Gubler and Hoffman (*10*) and plated for screening with probe UM1 (*11*). The nucleic acid sequence in Fig. 1 is a composite sequence obtained from overlapping clones obtained by this analysis.

Northern blot analysis (Fig. 2) with total poly(A)$^+$ RNA from five human and nine rat tissue or cell line sources indicated that the expression of uromodulin mRNA is tissue-specific. Of these sources, only kidney produced uromodulin mRNA, as indicated by the single hybridizing band of approximately 2.4 kb in rat and human kidney shown in a 4- and 30-hour exposure (*12*).

The quantity of uromodulin mRNA in kidney led us to search for previously described renal-specific proteins. We observed that purified uromodulin was recognized by a monoclonal antibody specific for the Tamm-Horsfall protein (*13*). Because amino acid sequence data were not available for the Tamm-Horsfall protein, a sample was prepared as described by Tamm and Horsfall (*14*). Amino acid sequence analysis of the intact Tamm-Horsfall protein and tryptic peptides of *S*-PE–Tamm-Horsfall protein revealed homology with the amino terminus of uromodulin, peptide sequences from tryptic peptides of uromodulin, and additional regions within the predicted primary structure of the uromodulin clone (Fig. 1). Furthermore, salt-precipitated Tamm-Horsfall and lectin-purified uromodulin had identical migration characteristics on SDS–polyacrylamide gel electrophoresis (PAGE) in both reduced and unreduced forms and yielded essentially identical patterns upon Western blot analysis (Fig. 3) (*1*).

For expression of uromodulin, a portion of the cDNA from nucleotide 73 to 2052 of the composite sequence (Fig. 1) was reconstructed by ligation into the Xba I and Sma I

Table 1. Antisense degenerate oligonucleotide probes for uromodulin. Probe UM1 was derived from tryptic peptide 1 and probe UM2 was derived from tryptic peptide 2 of the sequenced peptides in Fig. 1. Y is either C or T; R, A or G; K, G or T.

Probe	Sequence	Degeneracy	
UM1	Thr Leu Asp Glu Tyr Trp Arg		
	3'- GAY CTR CTY ATR ACC KC	32	
	3'- GAR CTR CTY ATR ACC KC	32	96
	3' AAY CTR CTY ATR ACC KC	32	
UM2	Phe Asp Lys Val Met Tyr		
	3'- AAR CTR TTY CAR AAR TAC AT		64
	3'- AAR CTR TTY CAY AAR TAC AT		

sites in the polylinker pUC19 (*15*). Transient expression of uromodulin in L cells with the expression vector UM312MO (*15*) yielded a protein that was specifically immunoprecipitated by antiserum specific for uromodulin and protein A Sepharose beads. Conditioned medium from the uromodulin transfection (lane 2, upper arrow head) contained polypeptides migrating with 97.4- and 200-kD markers (Fig. 3). The cell lysate (lane 4, lower arrow) contained slightly smaller specific bands. No immunoprecipitable polypeptides of these sizes were observed within the corresponding control lanes. Immunoprecipitation with a commercially available antiserum to Tamm-Horsfall protein gave the same result as the antiserum to uromodulin. The size difference between uromodulin secreted from the L cells and uromodulin in the cell lysate is thought to be due to differences in glycosylation. The less prominent band of larger molecular size (200 kD), which was specifically immunoprecipitated from conditioned medium and the cell lysate of L cells expressing uromodulin, may be a dimer caused by the reducing conditions used before gel electrophoresis.

Using the sequence homology screening program SEQHP, we compared the amino acid sequence of uromodulin with the protein sequence database of the protein identification resource sponsored by the National Biomedical Research Foundation (*16*). A screen of the entire database revealed that uromodulin exhibited significant sequence homology to eight sequenced proteins. Two proteins showed marked sequence homology: the murine epidermal growth factor (EGF) precursor, with a significance of 15 SD units, and the human low-density lipoprotein (LDL) receptor, with a significance of 9.5 to 10.9 SD units [calculated with the statistical program SEQDP (*16*)]. A lesser degree of homology was also noted with human and bovine clotting factors IX, X, and XII and with protein S. For both the EGF precursor and the LDL receptor, the homology was the result of a conserved cysteine-rich domain with the general sequence CXXXXXCXXXXXXXXCXC. Four homologous copies of this cysteine-rich sequence were noted in uromodulin at amino acids 32 to 63, 69 to 106, 112 to 148, and 297 to 335 (*17*). A potential cellular adhesion site with the sequence Arg-Gly-Asp was also noted beginning at position 142 (*18*).

Uromodulin binds with high affinity to murine recombinant IL-1α (rIL-1α) (*3*). We next screened for the ability of uromodulin to bind to other cytokines and growth factors. Uromodulin bound to plates coated with human rIL-1α, rIL-1β, and recombinant tumor necrosis factor (rTNF) (Fig. 4). Dose-response studies in the TNF ELISA (enzyme-linked immunosorbent assay) with concentrations of uromodulin from 10 μg/ml to 1 ng/ml showed that rTNF-coated plates exhibited half-maximal binding of uromodulin at 0.23 μg/ml (corresponding to 23 ng added to the ELISA plate) ± 0.03 μg/ml (mean ± SD; $n = 12$). Similar studies with rIL-1β–coated plates showed half-maximal binding at 2.7 ± 0.7 μg/ml ($n = 14$). Certain other cytokines might

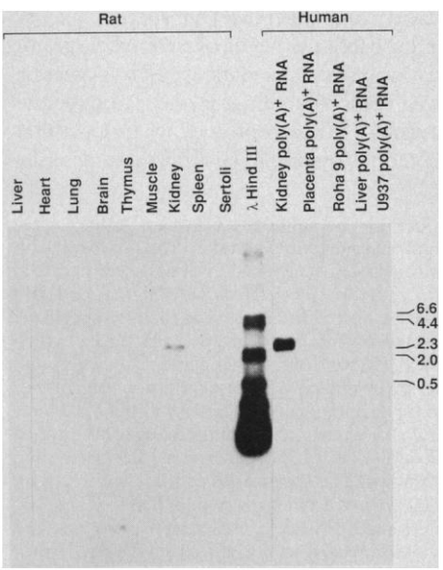

Fig. 2. Northern blot analysis of mRNA from rat and human sources (numbers to the right of the bands are kilobases). Northern blots containing 10 μg of total RNA (rat) or 1 μg of poly(A)$^+$ RNA (human) were hybridized to the ^{32}P-labeled uromodulin fragment (nucleotides 73 to 2052) in Fig. 1 (*8, 32*). The uromodulin cDNA fragment was labeled by random priming (*33*).

Fig. 3. (**Left two lanes**) Salt-precipitated Tamm-Horsfall glycoprotein (2 μg) and purified uromodulin (1 μg) separated on discontinuous SDS-PAGE with 12.5% acrylamide (*1*). Under unreduced conditions, both proteins migrated with an apparent molecular size of 85 kD. The proteins on the gel were then transferred to nitrocellulose and incubated with a high-titer rabbit antiserum against homogeneous uromodulin. Bound immunoglobulin G (IgG) was detected with biotinylated horseradish peroxidase–avidin–biotin complex (*1*). (**Right four lanes**) Immunoprecipitation of human recombinant uromodulin protein. Plates (100 mm) containing approximately 2×10^6 murine L cells were transfected with a control gene (BG301) and uromodulin cDNA (UM312MO) with the DEAE-dextran method with minor modifications (*34*). The conditioned medium was aspirated 48 hours after transfection, and the cells were washed twice with Hanks balanced salt solution. RPMI 1640 medium (3 ml) minus cysteine containing 1% dialyzed fetal calf serum (FCS) and 250 μCi of [^{35}S]cysteine per milliliter (~1000 Ci/mmol; NEN) was added, and the cells were incubated at 37°C until 50% of the label was depleted. RPMI 1640 medium (3 ml) containing 1% dialyzed FCS was added, and incubation continued for an additional 18 hours. At this point, labeled conditioned medium was harvested and the cells were lysed. Aliquots of the medium (1 ml) were immunoprecipitated with the antiserum to uromodulin. A commercial preparation of Tamm-Horsfall rabbit polyclonal antibody (Calbiochem) gave identical results. Immunoprecipitation and gel electrophoresis were performed as described (*3*).

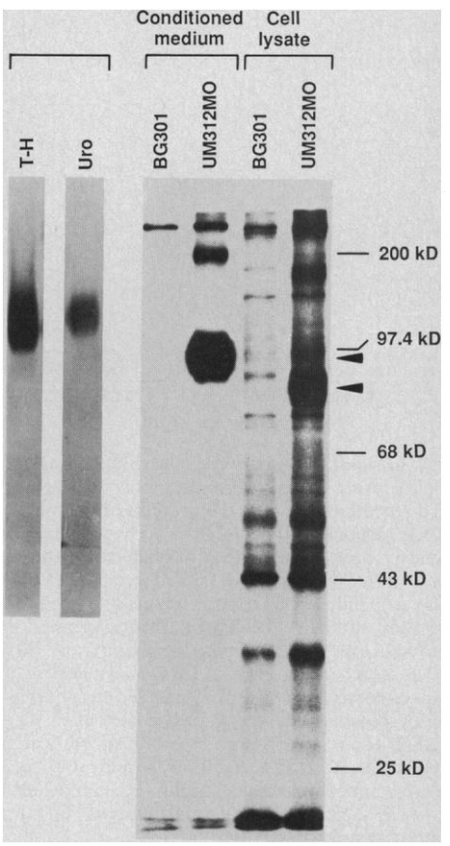

also exhibit specificity toward uromodulin; however, uromodulin is not just nonspecifically "sticky" because it did not bind to insulin, insulin-like growth factors, or bovine serum albumin. Also, uromodulin (up to 10 μg/ml) did not adhere to plates coated with transferrin, ceruloplasmin, fetal calf serum, or uncoated ELISA plates. Conversely, the binding of rIL-1 and rTNF appears to be specific for uromodulin because they did not bind to a number of other mammalian glycoproteins, such as α_1 acid glycoprotein, fetuin, and bovine submaxillary mucin. Finally, we have evidence that simple sugars can compete in binding uromodulin to human rIL-1α, rIL-1β, and rTNF (*19*). For example, 6-deoxy-D-galactose inhibits the binding of uromodulin to TNF-coated plates (50% inhibition, 80 m*M* sugar) and to IL-1–coated plates (50% inhibition, 20 m*M*). This finding is analogous to previous findings that murine rIL-1α appears to recognize a glycosylated site on uromodulin (*5*).

Because the tissue source of the Tamm-Horsfall glycoprotein is limited to the thick ascending limbs of Henle's loop and the early distal convoluted tubule, we examined tissue sections of human kidney for binding to antisera against homogeneous uromodulin (*20*). A uromodulin-specific antiserum brightly stained a subpopulation of renal tubules (Fig. 5). Identical staining was seen with a monoclonal antiserum raised independently against salt-precipitated Tamm-Horsfall glycoprotein (*13*). Our lymphokine-binding studies suggest a physiologic role for uromodulin; therefore, studies were performed to determine whether rIL-1 and rTNF could bind to these same renal tubules. Both rIL-1 and rTNF bound to the same area of renal tubules stained by antisera specific for uromodulin (Fig. 5, B to D). Although staining was specific for appropriate sections of the renal collecting system, other directly adjacent tubules distinct from the thick ascending limb of Henle's loop also stained with TNF and antiserum to TNF. Glomeruli, vascular tissue, and interstitial tissue did not stain, nor was tubular uptake seen in the absence of added IL-1 or TNF or with preimmune antiserum.

Since its original description, the function of the Tamm-Horsfall glycoprotein has been enigmatic. Because of its tendency to form precipitates, a number of investigators have examined its possible role in the formation of renal calculi; however, analyses of calculi show extremely variable concentrations of this glycoprotein (*21*). The effect of high concentrations of Tamm-Horsfall protein on assays of phytohemagglutinin-induced T-cell proliferation has also yielded conflicting results. One group found either no effect or stimulation of T-cell responses (*22*), and others found it to be inhibitory (*23*). On the basis of (i) identical migration after SDS-PAGE, (ii) immunologic identity on Western blot analysis, (iii) identical tissue distribution, and (iv) amino acid sequence identity, it is clear that uromodulin and the Tamm-Horsfall glycoprotein are identical.

Uromodulin, however, was originally described on the basis of its immunosuppressive activity in vitro. This activity does not require intact protein and is probably mediated by the carbohydrate portion of the molecule. We compared the in vitro biologic activity of eight independent batches of uromodulin isolated from urine of pregnant women by lectin adherence with that of eight batches of Tamm-Horsfall glycoprotein isolated by salt precipitation. In each case the material was homogeneous on SDS-PAGE. Half-maximal inhibition of antigen-specific T-cell proliferation by uromodulin was seen at 32 ng of material per culture, whereas the half-maximal inhibitory concentration of the Tamm-Horsfall was 414 ng per culture (*24*). Thus average inhibition by the Tamm-Horsfall glycoprotein was less than one-tenth that of uromodulin. In four of the eight batches, the salt-precipitated Tamm-Horsfall glycoprotein did not inhibit antigen-specific T-cell proliferation at any dose tested (up to 2 μg per culture). This difference was significant ($P = 0.04$) with a two-sample t statistic ($n = 16$; df = 14). Although the protein portions of the Tamm-Horsfall glycoprotein and uromodulin are identical, our data suggest that selection of concanavalin A–adherent material from urine of pregnant women yields substantially more immunoregulatory activity in vitro than salt-precipitated material isolated from sources other than pregnant women. This is consistent with the observation that the carbohydrate portion of uromodulin appears to be critical for biologic activity, and differences in specific activity are probably the result of differential glycosylation. Since our data strongly suggest a physiologic function for the carbohydrate portion of the glycoprotein, we propose that the term uromodulin be retained to describe

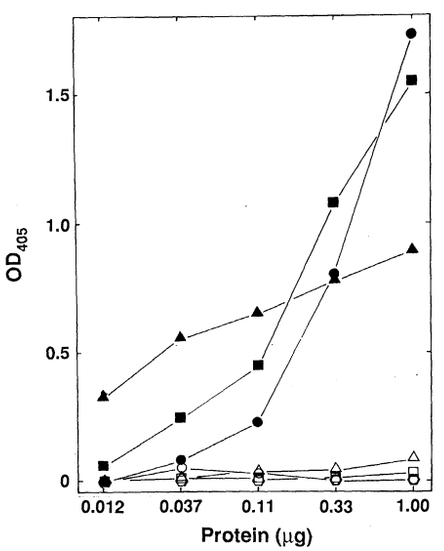

Fig. 4. Binding affinity of uromodulin. Immulon I plates were coated overnight with various purified recombinant or natural proteins (1 μg/ml) in 0.1*M* carbonate buffer (*p*H 9.6). They were then washed three times with phosphate-buffered saline (PBS) with added 0.05% Tween 20 (PBS-Tween), and various concentrations of uromodulin were added in PBS-Tween. Bound uromodulin was detected as described (*3*). Symbols: (■) TNF-coated plate, (●) IL-1β–coated plate, (▲) IL-1α–coated plate, (○) bovine serum albumin (BSA)–coated plate, (△) IGF-1–coated plate, (□) IGF-2–coated plate, and (◌) uncoated plate. IGF-1, IL-1β, IL-1α, and TNF were from bacterial recombinant sources; insulin, BSA, and IGF-2 were purified from natural sources. OD_{405}, optical density at 405 nm.

Fig. 5 (Opposite page). (**A**) Paraffin-embedded sections of uninvolved human kidney were deparaffinized in two 10-minute changes of xylene, and endogenous peroxidase was inactivated in methanol with 0.3% hydrogen peroxide for 30 minutes at room temperature. Slides were hydrated through graduated ethanol baths and equilibrated in PBS with 0.5% BSA (PBS-BSA; Sigma). A 1:100 dilution of the antiserum to uromodulin in PBS-BSA was incubated for 2 hours at room temperature. Sections were washed and then developed with a biotinylated antiserum specific for rabbit IgG and then by an avidin-biotinylated horseradish peroxidase complex (Vector Labs, Burlingame, California). No appreciable staining was seen with nonimmune rabbit serum or with any of the developing reagents. (B to D) Sections were first incubated with or without 100 ng of homogeneous rIL-1 or rTNF for 1 hour in PBS-BSA. IL-1 and TNF were detected with two different rabbit antisera against purified recombinant material. Antiserum to IL-1 detected bound IL-1 on ELISA plates at a 1:2000 dilution; antiserum to TNF detected bound TNF at a 1:1000 dilution. The specificities of these antisera were confirmed by Western blot analysis. Antiserum to IL-1β cross-reacted with bound IL-1α at a 1:100 dilution. Antiserum to TNF was used at a final 1:50 dilution in PBS-BSA; antiserum to IL-1 was used at a 1:100 dilution. Bound antiserum was detected with a biotinylated second antiserum system (Vector Labs). (**B**) rTNF (1 μg/ml) plus antiserum to TNF; (**C**) rIL-1β (1 μg/ml) plus antiserum to IL-1β; (**D**) antiserum to IL-1β in the absence of added IL-1. Slides treated with antiserum to TNF gave a similar background. Slides incubated with either rTNF or rIL-1β showed no appreciable staining either in the presence of preimmune rabbit serum or with only the developing reagents. Renal sections incubated with either rIL-1β or rTNF showed marked and specific staining that was localized to the thick limb of the ascending tubules in Henle's loop. Sections incubated with lymphokine had a higher and diffuse background. Furthermore, on high-power microscopic examination, the sections incubated with TNF appeared to stain not only thick ascending loop tubules but also tubules in close association with the thick ascending loop.

appropriately glycosylated protein able to bind to IL-1 and TNF and capable of suppressing antigen-specific T-cell proliferation in vitro.

That rIL-1 and rTNF bind to identical areas of the human kidney, which also stain with uromodulin-specific antisera, suggests that uromodulin may play a role in regulating the levels of these lymphokines. This hypothesis is strengthened by the observation that rIL-1 and rTNF bind to purified uromodulin in vitro. However, our data do not exclude the role of other cytokine-specific binding proteins, and renal sections incubated with rTNF appear to stain specifically not only the thick ascending loop tubules but also other immediately adjacent tubules that do not appear to bind antisera specific for uromodulin. The significance of this observation requires further study. The Tamm-Horsfall glycoprotein is present on all aspects of epithelial cells in the thick ascending limbs of Henle's loop and hence is in contact with the peritubular extravascular space. It might play a role in the transport of macromolecules from tubular lumen to peritubular capillaries, or vice versa (*25*). It is interesting that administration of ^{125}I-labeled TNF in vivo has demonstrated rapid and saturable renal removal of TNF from the circulation, suggesting a kidney-specific mechanism of TNF uptake (*26*).

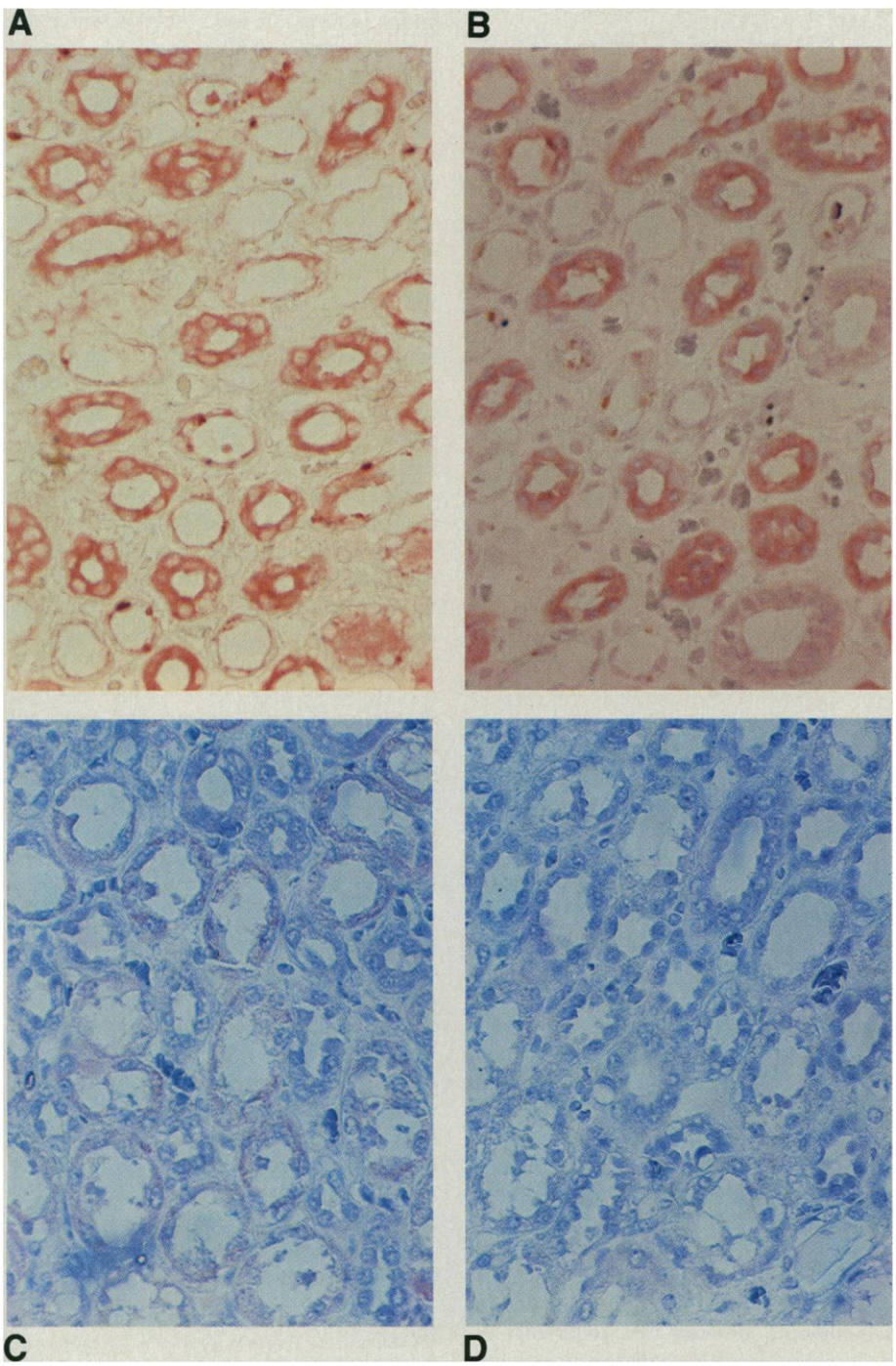

The uromodulin binding site on rIL-1 appears to be distinct from the IL-1 domain that binds to the IL-1 receptor found on T cells, B cells, and fibroblasts. The most direct evidence for this comes from studies with rIL-1β that had single amino acid substitutions introduced by site-specific mutagenesis (*27*). Mutations that affect binding to the cell surface receptor do not inhibit binding to uromodulin, and, conversely, single amino acid substitutions that block the binding of uromodulin do not interfere with binding to the cell surface IL-1 receptor (*28*). These and other results imply that IL-1 must have two separate binding sites, one responsible for binding to the previously described IL-1 receptor on T cells, B cells, and fibroblasts and the other exhibiting lectin-like specificity and having an affinity for uromodulin.

Our data suggest that a potential physiologic function of the Tamm-Horsfall glycoprotein (uromodulin) could be to act as a specific renal ligand for IL-1α, IL-1β, and TNF. Uromodulin may play an important role in regulating circulating levels of these lymphokines. Further, because of the lectin-like nature of the binding mechanism and the observation that, at least for IL-1β, the binding site to uromodulin is distinct from the cell surface IL-1 receptor, carbohydrate recognition may represent a general mechanism for the regulation of circulating cytokines. The kidney may therefore be a major immunoregulatory organ. Site-specific mutagenesis of the lymphokines or competitive inhibition of their carbohydrate-specific binding domains with defined carbohydrate antagonists could be used to regulate the circulating levels of the lymphokines.

Note added in proof: Pennica *et al.* (*29*) reported an identical amino acid sequence for uromodulin (Tamm-Horsfall glycoprotein).

REFERENCES AND NOTES

1. A. Muchmore and J. Decker, *Science* **229**, 479 (1985).
2. K. Brown *et al.*, *Proc. Natl. Acad. Sci. U.S.A.* **83**, 9119 (1986); K. Brown *et al.*, in preparation.
3. A. Muchmore and J. Decker, *J. Biol. Chem.* **261**, 13404 (1986).
4. A. Muchmore, *Am. J. Reprod. Immunol. Micro.* **11**, 89 (1986).
5. ———, S. Shifrin, J. Decker, *J. Immunol.* **138**, 2547 (1987).
6. A. Muchmore and J. Decker, *ibid.*, p. 2541.
7. J. Friedman *et al.*, *J. Biol. Chem.* **245**, 3868 (1970).
8. R. Cate *et al.*, *Cell* **45**, 685 (1986).
9. Probes UM1 (17 nucleotides, 96-fold degeneracy) and UM2 (20 nucleotides, 64-fold degeneracy) were labeled at their 5′ ends with polynucleotide kinase and [^{32}P]adenosine triphosphate before hybridization.

10. U. Gubler and B. J. Hoffman, *Gene* **25**, 263 (1983).
11. The initial screen of the library yielded 12 clones that hybridized to probe UM1 (Table 1). Results of DNA sequence analysis showed that the longest clone [4.3; 1800-bp insert] and an overlapping clone (4.4; 950-bp insert) contained an open reading frame but lacked an initiation codon and leader sequence. To obtain the additional missing 5′ sequence, the library was screened again with an antisense 30-nucleotide probe that corresponded to the 5′ end of clone 4.4. This yielded additional clones, including clone 6.7 that contains 105 nucleotides of 5′ untranslated region and encodes the putative initiating methionine, the leader sequence, and the mature amino terminus of the polypeptide.
12. A possible exception is rat heart, where a faint 2.4-kb band could be seen after a 3-week exposure of the blot.
13. S. Kumar *et al.*, *Histochem. J.* **17**, 1251 (1985).
14. I. Tamm and F. Horsfall, *J. Exp. Med.* **95**, 71 (1952).
15. This clone contains a portion of the 5′ untranslated region (32 bp), an open reading frame that potentially encodes a 24–amino acid leader, a 615–amino acid mature protein, and a portion of the 3′ untranslated region (26 bp). For transient expression in murine L cells, the gene was excised from pUC19 and inserted into the polylinker region of pBG312MO, an expression vector that contains the Moloney long terminal repeat in place of the SV40 early and adenovirus major late promoter region of pBG312 (*8*).
16. Both the SEQHP and SEQDP programs were developed by M. Kaneshia, Laboratory of Mathematical Biology, National Cancer Institute.
17. T. C. Sudhoff *et al.*, *Science* **228**, 893 (1985); J. Scott *et al.*, *ibid.* **221**, 236 (1983).
18. E. Ruoslahti and M. D. Pierschbacher, *Cell* **44**, 517 (1986).
19. A. Sherblom, J. Decker, A. Muchmore, in preparation.
20. E. Schenk, R. Schwartz, R. Lewis, *Lab. Invest.* **25**, 92 (1971); J. R. Hoyer *et al.*, *ibid.* **30**, 757 (1974).
21. A. M. Grant, L. R. I. Baker, A. Neuberger, *Clin. Sci.* **44**, 377 (1964).
22. J. S. Hunt and A. R. McGiven, *Immunology* **35**, 391 (1978).
23. A. Abbondanza *et al.*, *Biochem. J.* **187**, 525 (1980).
24. Half-maximal inhibition of antigen-specific T-cell proliferation was determined for the eight batches of uromodulin representing a total of 21 individual assays; similarly, the eight batches of Tamm-Horsfall glycoprotein were assayed a total of 14 times. If a preparation did not inhibit proliferation, it was arbitrarily assigned the highest value of uromodulin or Tamm-Horsfall protein tested (this ranged from 500 ng to 2 μg per culture). Since four of the eight Tamm-Horsfall preparations did not inhibit at any dose, this method yields a minimum estimate.
25. J. Hoyer and M. Seiler, *Kidney Int.* **16**, 279 (1979).
26. B. A. Beutler, I. W. Milsark, A. Cerami, *J. Immunol.* **135**, 3972 (1985).
27. H. R. MacDonald *et al.*, *FEBS Lett.* **209**, 295 (1986).
28. A. V. Muchmore *et al.*, in preparation.
29. D. Pennica *et al.*, *Science* **236**, 83 (1987).
30. A. M. Maxam and W. Gilbert, *Methods Enzymol.* **65**, 499 (1980).
31. G. M. Church and W. Gilbert, *Proc. Natl. Acad. Sci. U.S.A.* **81**, 1991 (1984); R. Tizard and H. Nick, unpublished information.
32. B. Wallner *et al.*, *Nature (London)* **320**, 77 (1986).
33. A. P. Feinberg and B. Vogelstein, *Anal. Biochem.* **132**, 6 (1983).
34. L. M. Sompayrac and K. J. Danna, *Proc. Natl. Acad. Sci. U.S.A.* **78**, 7575 (1981).

17 February 1987; accepted 15 May 1987

Saccharomyces cerevisiae Has a U1-Like Small Nuclear RNA with Unexpected Properties

PAUL G. SILICIANO, MICHELE HALTINER JONES, CHRISTINE GUTHRIE

Previous experiments indicated that only a small subset of the ≃24 small nuclear RNAs (snRNAs) in *Saccharomyces cerevisiae* have binding sites for the Sm antigen, a hallmark of metazoan small nuclear ribonucleoproteins (snRNPs) involved in pre-messenger RNA splicing. Antibodies from human serum to Sm proteins were used to show that four snRNAs (snR7, snR14, snR19, and snR20) can be immunoprecipitated from yeast extracts. Three of these four, snR7, snR14, and snR20, have been shown to be analogs of mammalian U5, U4, and U2, respectively. Several regions of significant homology to U1 (164 nucleotides) have now been found in cloned and sequenced snR19 (568 nucleotides). These include ten out of ten matches to the 5′ end of U1, the site known to interact with the 5′ splice site of mammalian introns. Surprisingly, the precise conservation of this sequence precludes perfect complementarity between snR19 and the invariant yeast 5′ junction (GTATGT), which differs from the mammalian consensus at the fourth position (GTPuAGT).

NUCLEAR PRE-MESSENGER RNA (mRNA) splicing is mediated by a set of small nuclear RNAs (snRNAs) (U1, U2, and U4 to U6) complexed with proteins that react with human autoimmune sera of the Sm specificity (*1*). The splicing reaction appears to be guided by specific small nuclear ribonucleoprotein (snRNP): intron and snRNP:snRNP interactions, the best characterized of which is that between U1 and the pre-mRNA. This interaction was first postulated 7 years ago based on the striking complementarity between the 5′ ten nucleotides of U1 and the conserved sequence found at metazoan 5′ splice junctions (*2*). Subsequent data from in vitro splicing systems have provided persuasive support for this model (reviewed in *3*). Furthermore, Zhuang and Weiner (*3*) recently demonstrated base pairing at two of the ten positions by constructing base changes in U1 to compensate for point mutations in the 5′ junction.

We have previously identified snRNAs in *Saccharomyces cerevisiae* by criteria that include possession of a characteristic trimethylguanosine (TMG) cap (*4*). In contrast to our expectations from work in higher eukaryotes (i) yeast snRNAs are present in relatively low abundance (10 to 10^3 copies per cell in yeast versus 10^5 to 10^6 in mammalian cells) (*5*); (ii) the yeast snRNA family contains at least two dozen species, some of which are quite large (up to six times the largest metazoan snRNA) (*4*); and (iii) at least six of these are dispensable for growth (*6*).

In order to identify yeast snRNAs likely to function in mRNA splicing, we looked for those RNAs that were associated with Sm proteins. Because reported attempts to immunoprecipitate snRNAs from whole cell sonicates with antibodies to the Sm proteins (anti-Sm) were unsuccessful (*7*), we used the alternative approach of microinjecting ^{32}P-labeled yeast snRNAs into *Xenopus* oocytes (*8*), which stockpile the Sm protein (*9*). We reasoned that if any yeast snRNAs contained Sm binding sites (*10*), they would assemble into Sm-snRNPs and become immunoprecipitable. By this assay, two snRNA species, snR7 and snR14, were detected after immunoprecipitation with human antibodies (*8, 11*). We have since demonstrated that snR7 (179 nt) has limited sequence-specific but strong structural homology to U5 (116 nt) (*12*), while snR14 (160 nt) has several blocks of sequence homology to U4 (144 nt) (*13*). By sequence analysis, snR7 and snR14 each contain a consensus Sm binding site ($AU_{5\text{-}6}$ GPu). Moreover, both RNAs are essential for viability (*12, 13*) and can be found in association with the spliceosome (*14*). This is also true for a third snRNA, snR20 (1175 nt; also called LSR1) (*14*), which has a 5′ domain of striking sequence and structural homology to U2 (187 nt), including a presumptive Sm binding site (*15*).

These results suggested that, despite differences in size and structure, yeast might contain a full complement of functional analogs to the Sm snRNPs of higher eukaryotes, including the U1 counterpart. Trivial explanations, such as degradation, could account for the failure of species other than snR7 and snR14, including snR20, to be efficiently immunoprecipitated after microinjection. We now have turned to direct analysis of yeast snRNPs. Knowing that yeast snRNAs are much less abundant than their mammalian counterparts (*4, 5*), we have used active splicing extracts as starting material because these are likely to be enriched for the snRNPs of interest.

Extracts were prepared and incubated in the presence of protein A–Sepharose that

Department of Biochemistry and Biophysics, University of California, San Francisco, CA 94143. The order of the first two authors is arbitrary.